EDDY CURRENT TESTING

Eddy current testing is a nondestructive evaluation method that is based on the principle of electromagnetic induction. While an alternating current passes through a coil, an alternating magnetic field is produced that is oriented perpendicularly to the direction of the current and parallel to the axis of the coil. If a conductive object is located in proximity to the coil, circular eddy currents will be induced within its surface layer normal to the magnetic field. Eddy currents in turn generate a secondary magnetic field that is in opposition to the primary coil field. The interaction between the two fields causes a partial decreasing of the primary field, hence a change in coil impedance or coil voltage. Therefore, a coil and a conductive object close to each other couple into a unified system through the interaction of alternating current in the coil and the induced eddy current in the body. A schematic representation of the system is shown in Fig. 1. Essentially, the eddy current testing means to measure the change of coil impedance (1). The magnitude of the coil impedance is related to either the coil construction or the coupling strength between the coil and tested object. The coupling strength is affected by a number of factors, such as electrical conductivity σ, magnetic permeability, μ of the object (target) material size, shape, and the distance (or clearance) x between the coil and object. Coil construction parameters include outer diameter D, inner diameter d, thickness b, and the number of turns w, and are designed according to particular testing requirements. They are all the factors that affect the magnitude of coil impedance, but they are always kept constant after the coil, the eddy current probe, is built up.

When the object is machined of homogeneous metallic material, and the conductivity σ, permeability μ, and its shape and dimensions are all fixed, then changes in magnitude of the coil impedance vary with changes in the distance x. This phenomenon is called *lift-off effect* (2). Based on lift-off effect, an eddy current transducer provides displacement measurement; hence, we can measure vibration, motion trace, metal foil and sheet thickness, and thickness of cladding material, either for nonmetal plating on metal material or for a nonmagnetic layer on magnetic material.

If the distance x is kept stationary, the magnitude and changes in coil impedance indicate the combined influences of conductivity σ and permeability μ of the object material, upon which flaw detections are possible. When the permeability μ is also fixed, the coil impedance becomes a function of the conductivity σ. Thus one could determine the impurity con-

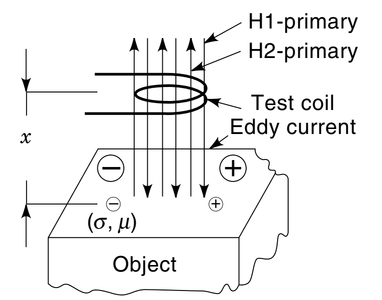

Figure 1. Eddy current principle. I_1 is the exciting ac current; x the distance between coil and tested object; σ, μ are the conductivity and magnetic permeability of the object material, respectively.

tent of pure metal, heat treatment condition of an alloy, concentration of dielectric medium, etc. But otherwise, with conductivity σ fixed, impedance will vary with permeabilities, and one could inspect grain-size metallic materials, thermal related strain, hardness, and so on. Therefore eddy current testing is a multivariable detecting technology and has extensive usage. Some major applications will be stated later.

Eddy current was discovered in 1824 when Gambery (3) noted the eddy current damping phenomenon when the oscillations of a suspended bar magnet rapidly stopped whenever a copper plate was held under it. Subsequently, many scientists dedicated themselves to the study of eddy current theory and its practical use; however, progress was very slow. Förester first investigated the influence of radial cracks in a metal bar on coil impedance in 1954 (10). Dodd and Deeds (11) in 1968 and Libby (4) in 1971 successfully put forward a theory for analytically calculating the induced eddy current within the cross section of a metal bar in an ac magnetic field, eddy current technology has developed rapidly. Now, numerous versions of eddy current test equipment as nondestructive measurement tools have been successfully developed and are commercially available (2).

Eddy current testing has many advantages, such as the following:

1. A probe coil need not contact the tested object (specimen).
2. It has high sensitivity for measuring the surface or subsurface of conductive materials.
3. It has a fast response—can be used for either static or high-speed dynamic testing.
4. It is unnecessary to have some actuating medium between probe and specimen. Neither is there a problem even if dust, oil, or any other nonmagnetic and primarily non-conductive medium gets between them. Therefore, eddy current testing can be done in unsatisfactory conditions.
5. A variety of testing circuits, such as bridge circuits, resonant circuits, feedback circuits, and phase discriminators are available to generate corresponding outputs of voltage, current, phase, or frequency to reflect coil impedance and its changes.

Just as everything has strengths and weaknesses, however, the eddy current testing method does have inherent limitations (12), as follows:

1. It is applicable only for testing of conductive materials.
2. It detects flaws mainly for surfaces or surface layers, but cannot determine the shape and types of flaws.
3. It is difficult to inspect specimens with complex shape.
4. Eddy current testing can be used to deal with multiple variables; however, this very advantage can bring about interference signals in the results, so that special signal processing is often necessary.

PRINCIPLES OF EDDY CURRENT TESTING

The impedance of an eddy current coil can be analyzed under three distinct conditions (5).

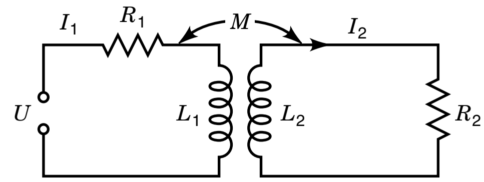

Figure 2. Equivalent circuit of the coil coupled with a conducting object.

Idling Impedance

This is the coil impedance with tested object very far from the coil, thus not influencing its impedance. Idling impedance Z_0 is

$$Z_0 = R_1 + j\omega L_1 \tag{1}$$

where R_1, L_1 are the resistance and inductance of the coil, respectively (Fig. 2), and ω is the angular frequency ($\omega = 2\pi f$).

First-Stage Impedance

The impedance of a coil coupled with an object of known physical properties is defined as *first-stage impedance.* It indicates the characteristics of a coil impedance that varies with the distance between coil and object, such as lift-off effect. As mentioned previously, when a metal specimen is placed adjacent to a coil carrying an alternating current, secondary or eddy current will be induced within the surface layer of the specimen. Figure 2 shows the equivalent circuit. According to Kirchhoff's voltage law, a set of equations can be written:

$$(R_1 + j\omega L_1)I_1 - J\omega M I_2 = U \tag{2}$$

$$-j\omega M I_1 + (R_2 + j\omega L_2)I_2 = 0 \tag{3}$$

where R_2, L_2 are resistance and inductance of eddy current loop in tested specimen. M is the mutual inductance between the coil and the tested specimen. From Eqs. (2) and (3), the first-stage impedance Z of the coil can be derived:

$$Z = \left[R_1 + \frac{\omega^2 M^2 R_2}{R_2^2 + (\omega L_2)^2}\right] + j\omega\left[L_1 - \frac{\omega^2 M^2 L_2}{R_2^2 + (\omega L_2)^2}\right] \tag{4}$$

The equivalent resistance R of the coil is a function of the mutual inductance M:

$$R = R_1 + \frac{\omega^2 M^2 R_2}{R_2^2 + (\omega L_2)^2} \tag{5}$$

Obviously, R increases with the decreasing distance between coil and object. Note that this variation is independent of material characteristics (magnetic or nonmagnetic). From the second term of Eq. (4), the equivalent inductance L of the coil is

$$L = L_1 - \frac{\omega^2 M^2 L_2}{R_2^2 + (\omega L_2)^2} \tag{6}$$

L is influenced by two physical effects. The first term L_1 is related to magnetostatic effects, so that it is dependent on whether the material is magnetic or nonmagnetic. The second term $\omega^2M^2L_2/[R_2^2 + (\omega L_2)^2]$ is generally considered as a reflected inductance caused by eddy current effect. The result of these two effects on equivalent inductance L is opposite. When the distance between coil and specimen decreases, coil inductance L increases as a consequence of magnetostatic effect, but it decreases, because of eddy current effect. Based on the analysis above, we can relate the variation in distance between coil and specimen to the variation of impedance.

Secondary Stage Impedance

Here we define the impedance of a coil adjacent to an object of unknown physical properties as *secondary stage impedance.* It demonstrates characteristics of coil impedances as related to tested objects that have different physical properties. In nondestructive testing, it is necessary to gain information about conductivity, permeability, and various flaws, so the concept of secondary stage impedance was born at the right moment. From Eq. (5), the resistance increment ΔR of equivalent resistance of a coil is

$$\Delta R = \frac{\omega^2 M^2 R_2}{R_2^2 + (\omega L_2)^2} \tag{7}$$

And from Eqs.(4) and (6), the reactance increment $\omega\Delta L$ of equivalent reactance of the coil is

$$\omega\Delta L = \omega\frac{\omega^2 M^2 L_2}{R_2^2 + (\omega L_2)^2} \tag{8}$$

When we divide Eq. (7) by Eq. (8), we obtain

$$\frac{\Delta R}{\omega\Delta L} = \frac{R_2}{\omega L_2} \tag{9}$$

The resistance increment ΔR and inductance increment ΔL of the eddy current coil generally depend upon metal conductivity. When the mutual inductance M is selected as a fixed value and ωL_2 is assumed as a constant, Eq. (9) tells us that there are different ratios of $\Delta R/\omega\Delta L$ for different metals. This is the theoretical basis of measuring metal conductivities. If we take the increments ΔR and $\omega\Delta L$ as horizontal and vertical axes, respectively, an impedance information graph (showing the relationships of $\omega\Delta L$ and ΔR in impedance Z) can be drawn by plotting $\omega\Delta L$ against ΔR (5). The slope of the plotted straight line is $\omega L_2/R_2$. Figure 3 shows that different conductivities of tested objects have different lines. Here we see that the particular exciting angular frequency ω is very critical. Too high a frequency is unsuitable for measuring metallic conductivity. Using Eqs. (7) and (8), we can eliminate R_2; then we have

$$(\Delta R)^2 + \left(\omega\Delta L - \frac{M^2\omega}{2L_2}\right)^2 = \left(\frac{M^2\omega}{2L_2}\right)^2 \tag{10}$$

Equation (10) shows that when the angular frequency ω and mutual inductance M are fixed at certain values, the impedance information graph follows semicircle law. The center of the semicircle sits in the vertical axis of $\omega\Delta L$, its radius is $M_2\omega/2L_2$. Different semicircles can be plotted for different M. Each semicircle passes through the origin of the coordinates

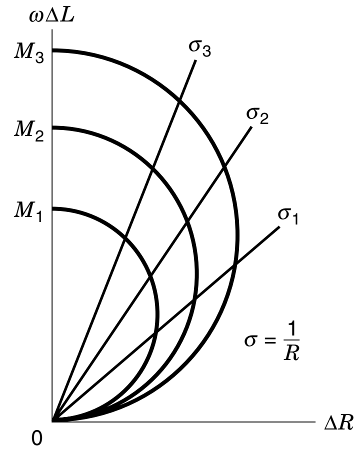

Figure 3. Relationships between metallic conductivity and information impedance.

and is tangential with the horizontal axis (ΔR axis). For a particular metal conductivity and mutual inductance, the intersecting point of the above straight line and the circle shows the value of the coil impedance information precisely.

The impedance diagram is the basis of eddy current testing. The relationship between coil impedance and flaws, cracks, lift-off, conductivity, permeability, and frequency, as well as the degree of filling, can be clearly known from the impedance diagram (2). Now, we let R be the horizontal axis and ωL the vertical axis, resulting in a complex impedance plane in which the terminal locus of impedance Z becomes the impedance diagram (6). It is the advantage of the complex plane diagram that the locus is rather clear and readily perceived, as shown in Fig. 4(a). We find that the shapes of loci are similar to each other, but their magnitudes and positions are much different, being affected by different radii of coils and exciting frequencies. Therefore this kind of impedance diagram is difficult to study and utilize. In order to overcome this limitation, a normalized impedance diagram is usually

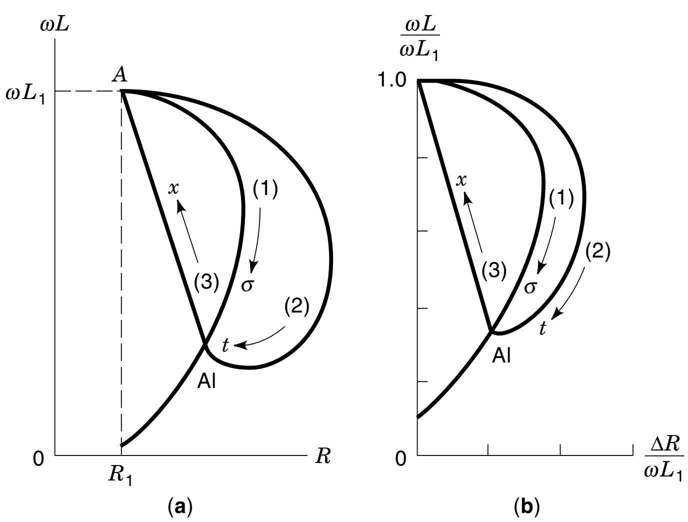

Figure 4. Impedance diagram of aluminum. (a) Impedance changes with variables. (b) Normalized impedance diagram. (1): Conductivity σ. (2): Thickness t. (3): Clearance (lift-off distance) x.

used. As shown in Fig. 4(a), this normalization is achieved first by moving the vertical axis right to the idling coil resistance, R_1, eliminating the left part of the information impedance with the tested object free. Then the two coordinate axes are divided by the idling coil reactance ωL_1. Through this modification, normalized impedance diagrams are the same no matter what the exciting frequency and radii of coils are changed to (5), as shown in Fig. 4(b). The fractional resistance $\Delta R/\omega L_1$ and reactance $\omega L/\omega L_1$ are all dimensionless and all less than 1. Therefore normalized diagrams have identical forms and are extensively comparable.

In eddy current testing, there are many variables that cause changes in coil impedance, and so it is very complicated to analyze their influence. For simplification, Förester proposed a conception of *effective permeability.* He assumed an ideal model in which a cylindrical tested object is placed in an infinitely long solenoid coil that carries ac current. A constant field exists at any cross section of the cylinder, but magnetic permeability changes in the section along its radial direction. However, the related magnetic flux equals that in the real cylinder. Under these assumptions, he came to a conclusion that the real alternating magnetic intensity and constant permeability could be replaced by a constant magnetic intensity and an alternating permeability. This assumed altering permeability is called *effective permeability,* symbolized as μ_{eff}, and is defined by the equation

$$\mu_{\text{eff}} = \frac{2}{\sqrt{-j}} \cdot \frac{J_1(\sqrt{-j}kr)}{J_0(\sqrt{-j}kr)} \tag{11}$$

where $K = \sqrt{\omega\mu\sigma}$, r is the radius of the cylinder, $J_0(\sqrt{-j}kr)$ is a zero-order Bessel function, and $J_1(\sqrt{-j}kr)$ is a first-order Bessel function. After introducing the concept of effective permeability, Förester defined the frequency at which the modulus of the Bessel function argument (kr) equals 1 as the *character frequency* f_g and called it the *limiting frequency* (2):

$$f_g = \frac{1}{2\pi\mu\sigma r^2} \tag{12}$$

Obviously, for a common testing frequency f, the following equation is valid:

$$kr = \sqrt{2\pi f\mu\sigma r^2} = \sqrt{f/f_g} \tag{13}$$

Effective permeability μ_{eff} changes with variable (kr), so μ_{eff} can be calculated as long as the ratio of f/f_g is known. Conventionally, f/f_g is taken as a parameter for the analysis of coil impedance.

In practical eddy current testing, a tested cylinder with diameter d usually cannot fully fill the testing coil, which has an inner diameter D, because a gap between coil and tested object is needed for relative movement. Here we define the fill factor η (1) as

$$\eta = (d/D)^2 \tag{14}$$

Undoubtedly, the influence of a tested object with different η on coil impedance is different.

From the analysis above, the effect on coil impedance of the opposing magnetic field produced by eddy currents in tested objects is completely determined by the fill factor η and effective magnetic permeability μ_{eff}. On the other hand, we can see from Eqs. (11) and (13) that μ_{eff} is determined by the ratio of f/f_g. Therefore the variation of coil impedance is actually determined by factors η and f/f_g. Thus, for a constant value of η, the distribution of eddy current and magnetic flux density in tested objects is a function of f/f_g. This result leads to a new conclusion: For two different tested objects, if η is kept constant and the corresponding frequency ratios f/f_g are the same, then the geometric distribution of effective permeability, eddy current density, and magnetic flux density are also the same, respectively. This is the so-called *law of similitude* of eddy current testing (5). From Eq. (13) the similitude condition can be written as

$$f_1\mu_1\sigma_1 r_1^2 = f_2\mu_2\sigma_2 r_2^2 \tag{15}$$

where the subscripts 1 and 2 describe the physical parameters and geometric sizes of tested bodies 1 and 2, correspondingly.

The law of similitude is a theoretical basis for proper simulation experiment. When problems that are solved neither by mathematical method nor settled by direct measurement are encountered in eddy current testing, we can have reasonable results according to the law by simulation experiment. For example, the law of similitude is applied to detect discontinuity flaws of materials, as long as the frequency ratios f/f_g are equal, and discontinuity flaws with geometric similarity (such as flaws having definite depths and widths that are all described as percentages of the cylinder diameter) will cause equal eddy current effect and equal variation of effective magnetic permeability. So, by means of a simulation test model with artificial flaws, the relationship between the variation $\Delta\mu_{\text{eff}}$ of effective permeability and the depth, width, and location of the flaw can be demonstrated. According to the similitude law, we can take these well-established results as a valid basis for practical evaluation of existing flaws. Thus, in testing of metal wires and small-size tubes, the influences of cracks on the probe coil's parameters may be understood by study of a test model with a magnified cross section and artificial flaws. Fortunately, in the testing of large tubes with eccentricities, nonuniform wall thickness, as well as other flaws, simulation testing makes the evaluation much easier. For particular applications, impedance plane diagrams are usually drawn with selected f/f_g as a parameter. Experimental results indicate that frequency ratios f/f_g within the range of 5 to 150 are of high sensitivity and practical significance.

Eddy Current Probe

The eddy current probe is one of the key components in eddy current testing equipment (2). It consists of a sensing coil, a coil frame, and connecting cables. Performance of the coil directly affects testing accuracy and data reliability. Figure 5 shows several types of eddy current probes for testing metallic tubes, cylinders (wire), and planar objects.

APPLICATIONS OF EDDY CURRENT TESTING

Applications of eddy current testing are generally classified into three main kinds: nondestructive flaw detection, material examination, and displacement and vibration measurement.

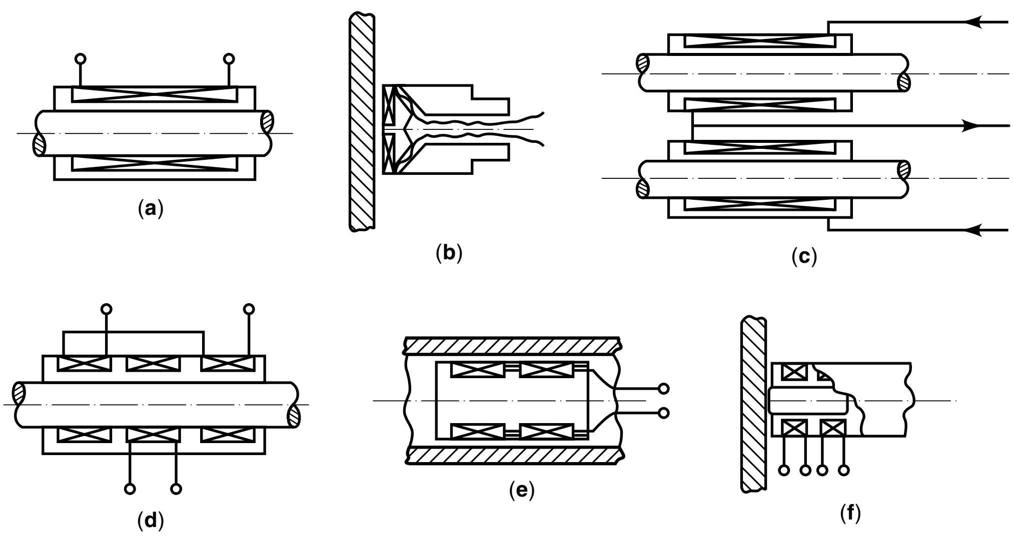

Figure 5. Several designs of eddy current probes. (a) Solenoid-type coil (or single coil) around cylindrical specimen, absolute measurement. (b) Pancake-type coil (or surface-mounted type probe) for testing planar objects. (c) Double coils for comparison measurement. (d) Multi-solenoid coils for differential measurement. (e) Bobbin probe (double or multiple coils) for use in tubular specimen. (f) Pancake-type coils with ferrite cores, the front coil used as a sensing coil, the rear for temperature compensating.

Nondestructive Flaw Detection

Flaw Detection in Metallic Tubes. The main purpose of tube flaw detection is to understand flaw kinds, their geometric shapes, and their locations. However, it is difficult to calculate theoretically the sites and shapes of flaws (13). Simulation tests, as pointed out before, are available to acquire knowledge about various flaws (such as shapes, sizes, and locations) within different materials under different ac exciting frequencies. The resulting data, tables, and curves can provide reference criteria for other practical testing (14). For that reason, reference specimens with standard artificial flaws, called *standard scars,* are necessary. Figure 6 shows four types of artificial flaws.

With wide use of eddy current testing, standardization of artificial flaws in many countries is increasingly accurate (8). A number of symbols, shapes, and sizes of standard flaws has been clearly designated today, making the selection, application, and reproduction of artificial flaws much easier. For the testing of tubular materials, single-coil solenoids are often employed. With reference to wall thickness, tubular materials can be put into two categories: thin-walled tubes and thick-walled tubes. The influence of tubular material on coil impedance is determined by the conductivity σ, relative permeability μ_r, outer and inner diameters d_2 and d_1, and wall thickness w. Of course, flaws within the outer and/or inner surface of a tube and eccentricity are also factors that affect coil impedances. Figure 7(a) shows that impedance varies with outer diameter d_2 (η is altered), whereas the ratio of d_2/d_1 is kept constant and the impedance diagram presents a set of semicircular curves in the case of η = 1, 0.75, 0.5, respectively. Each of the curves indicates coil impedance changes with conductivity σ, inner diameter d_1, and wall thickness w; and with frequency ratio of f/f_g under the condition of outer diameter d_2 = constant (η is fixed). The crosswise-oriented curves indicate direction of the variation in coil impedance with outer diameter d_2.

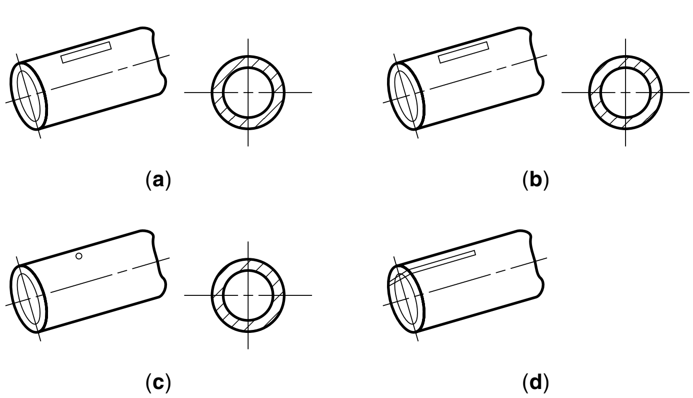

Figure 6. Several types of artificial defects. (a) Rectangle slot. (b) V-type slot. (c) Hole (or blind hole). (d) "Wire cutting" gap.

If the inner diameter d_1 of the tubular material is fixed, variation of outer diameter d_2 may cause two types of effects: One is outer diameter effect, where the crosswise curve in Fig. 7(a) shows the changes of impedance. The second is wall thickness effect, which makes f/f_g change greatly while the impedance value reaches to a new place corresponding to the new point of f/f_g. Because these two effects happen at the same time, impedance variation along with the crosswise curve caused by outer diameter effect is not very obvious, but it changes clearly along the semicircular curve symbolized as f/f_g. So the "total effect" makes impedance vary along the curve labeled, "varying d_2 and w" as shown in Fig. 7(b).

The eddy current effect of cracks in thin-wall tubes is the same as that of decreasing w of wall thickness. Therefore the effect owing to the existence of cracks in the outer surface layer is identical to that caused by altering outer diameter d_2 while inner diameter d_1 remains fixed–see Fig. 7(b). Simi-

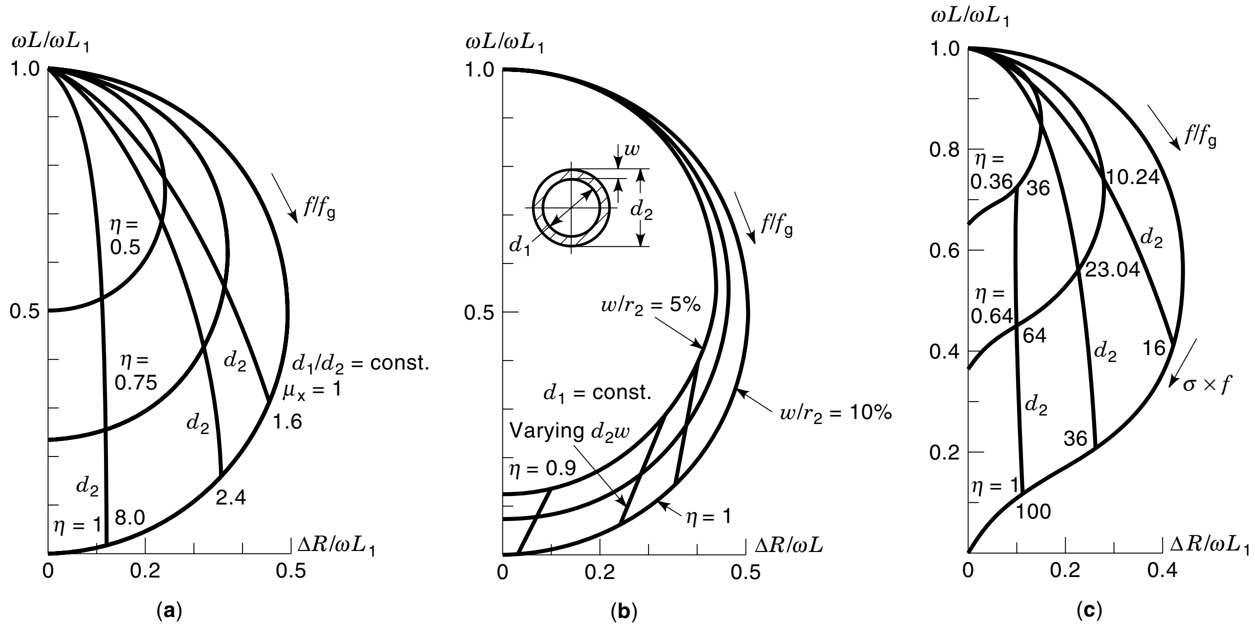

Figure 7. Impedance diagram for nonmagnetic thin wall tubes. (a) Coil impedance changes with d_2 as d_1/d_2 = const. (b) Coil impedance changes with d_2 as d_1 = const. (c) Coil impedance changes with d_2 as d_1/d_2 = 80%.

larly, the effect caused by cracks in the inner surface layer is identical to that caused by altering inner diameter d_1 while outer diameter d_2 is kept constant (wall thickness w varies), as shown in Fig. 7(a).

A frequency range corresponding to $f/f_g = 0.2 \sim 2.4$ is usually selected as the exciting frequency because there is greatest sensitivity at the point of $f/f_g = 1$.

Impedance curves of single coil testing of thick-walled tube are located, in the impedance diagram, between curves tested from cylinders and thin-walled tubes. If the ratio of d_1/d_2 of a thick-walled tube holds constant, whereas the outer diameter d_2 changes, we will obtain the impedance diagram shown in Fig. 7(c). Figure 7(c) also shows a set of curves for coil impedance that varies with frequency ratio f/f_g under the condition of d_1/d_2 = 80% and η (or d_2) as a parameter. As the outer diameter changes, the coil impedance changes chordwise.

For understanding of interior flaws, a great amount of model testing is necessary (5). Figure 8 shows the effects of cracks in nonmagnetic tubes, localized at different sites and depths, on coil impedance at frequency ratios f/f_g = 5 and 15. We can see from the diagram that there is a phase shift between impedance curves of cracks in inner and outer walls and the impedances increase with f/f_g and w/r_2. The effect of cracks within the material on the coil impedance is slightly less than that of cracks having the same depths in the inner or outer surface layer.

In practical applications, single coil testing is generally employed for tubes with diameters smaller than 75 mm, whereas the bobbin-type coil is suitable for tubes with diameters larger than 75 mm. Usually, a single-pancake coil or surface-mounted probe is preferable for tubes with very large diameters.

Flaw Detection in Metallic Rods and Wires. Even though eddy current testing can only detect flaws in the surface or surface

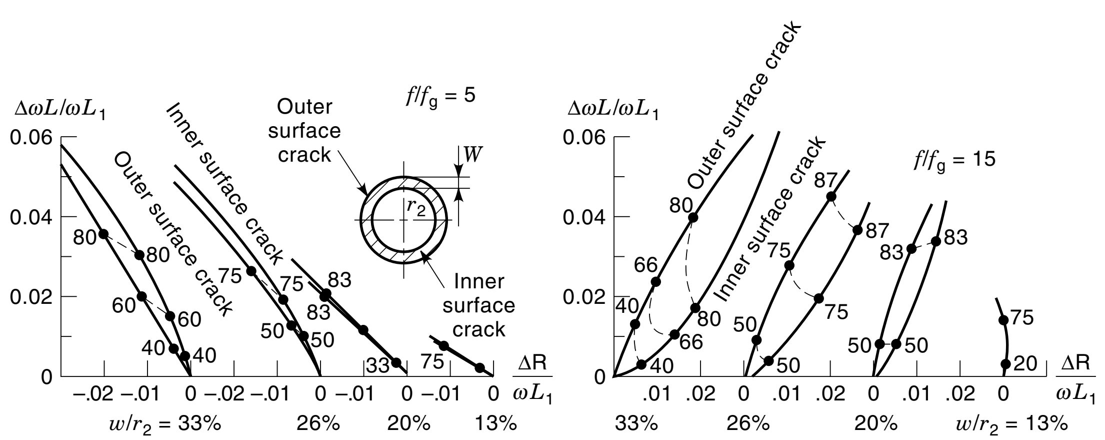

Figure 8. Coil impedance affected by cracks in nonmagnetic metal tube. Numbers on curves represent the depth of cracks as percent of wall thickness, *W*.

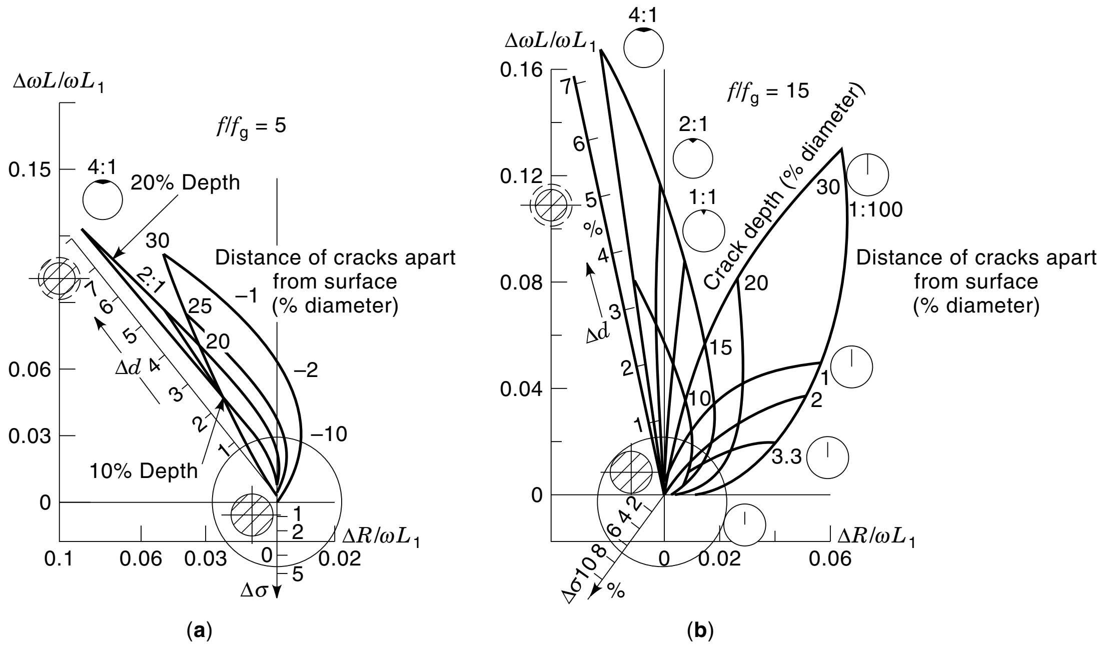

Figure 9. Cracks' effect on solenoid coil impedances. (a) $f/f_g = 5$. (b) $f/f_g = 15$.

layers, it is widely used in the area of surface quality evaluation for some metallic rods and wires. For flaw detection of the batch process rods and wires, a similar way to detect flaws in metal tubes is available. However, eddy current penetration is smaller in rods and wires than in tubes, and its distribution is also different. In order to raise eddy current sensitivity, a much lower test frequency should be selected than that used for tube testing (5). For these applications, single coil may often be used as the detecting coil.

As mentioned in the last section, the conductivity σ, magnetic permeability μ, dimensions and flaws of tested materials, and testing frequency are the major factors that influence coil impedances. The effect of flaws on coil impedance can be considered as the combined result of conductivity and dimensions. Flaws that are characterized by such qualities as their shape, depth, and location are very difficult to calculate theoretically. Hence flaw detections currently have to be achieved by means of model testing.

Figure 9 shows the effects of flaws on coil impedance and the curves resulting from model tests at frequency ratios of $f/f_g = 5$ and 15 for nonmagnetic cylinders (rods) with flaws of various locations, shapes, depths, and widths. The zero points of all these curves relative to flaw-free objects are located at the point that is determined by the frequency-dependent effective permeability μ_{eff}.

With $f/f_g = 15$, for example, one line segment marked Δd on Fig. 9(b) expresses the "diameter effect" relative to variation of diameter, and the numbers on it indicate percent decrease in diameter. Another line segment marked $\Delta\sigma$ expresses the "conductivity effect," and the numbers indicate percent increase in conductivity. Other line segments marked 10, 15, 20, and 30 show the regularity of coil impedance variation in the case of a tested cylinder with narrow cracks and width-to-depth ratio of 1 : 100 and when depths equal 10%, 15%, 20%, and 30% of diameter, respectively. The numbers 3.3, 2, and 1 at the right-hand side express the distance of upper terminals of internal cracks to the object (cylinder) surface as being 3.3%, 2%, and 1% of diameter. The numbers 4 : 1, 2 : 1, 1 : 1 express width-to-depth ratios of cracks. We also can see from the diagram that, for a subsurface crack with a depth of 30% diameter, as its upper terminalis gets farther from the surface, the coil impedance will vary along the curve marked with the numbers 1, 2, and 3.3. When the depth of a "V-type" crack varies, the coil impedance will vary along the curve marked with the ratios 4 : 1, 2 : 1, and 1 : 1. Furthermore, with the increasing width-top-depth ratio, the orientation of *crack effect* becomes that of *diameter effect.* According to the analysis above, the danger of cracks can be evaluated. For instance, the larger the angle included between the directions of crack effect and diameter effect, the deeper the crack. A harmful "sharp crack" is often the case. Otherwise, the heavy scratch mark usually has a large width-to-depth ratio, but the included angle between crack and diameter effect is very small or near zero, so it does not cause any danger.

In practical eddy current nondestructive crack detections, a frequency ratio f/f_g ranging from 5 to 150 is valuable. The optimum ratio for searching surface cracks is within 10 to 50. And a ratio of 4 to 20 is the best range for searching for subsurface cracks, whereas a ratio of 5 to 10 is useful for detecting both surface and subsurface cracks (5).

Material Examination

Eddy current testing of materials is achieved by measuring the variations of electrical conductivity and magnetic permeability of tested objects (9). Usually, material quality condition such as chemical constitution and impurity content affect conductivity and permeability.

Determining Chemical Composition and Impurity Content of Nonmagnetic Metals. The relative permeability μ_r for nonmagnetic metallic material is $\mu_r = 1$, approximately that of air,

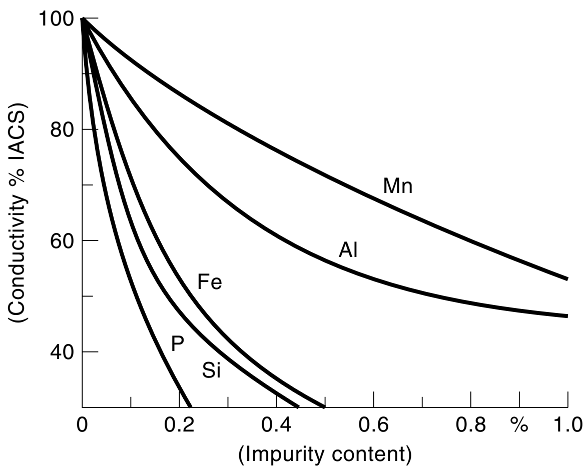

Figure 10. Effect of impurity content on copper conductivity.

and it is generally taken as constant. Therefore, the problem is simplified because only conductivity need be measured by the eddy current method.

The purity of metallic materials is closely related to their conductivities. If a small amount of impurities is melted into the materials, their conductivities will be decreased rapidly. Figure 10 shows the variation of electrical conductivity of metallic copper with different impurities and different content amounts. We can see from the diagram that even if the impurity contents in copper are 0.1% to 0.2% Fe, Si, or P, and so on, the conductivity decreases dramatically. Furthermore, the variation of conductivity is roughly proportional to the impurity content. Here unit IACS in diagram is the international annealed copper standard (6). Conductivity of copper according to it is defined as 100% IACS. In the copper industry, the amount of impurity is evaluated by its conductivity.

In brief, once we obtain the definite relationships between conductivities and impurity content, we can easily conclude what impurities and how much of them the material contains.

Determining Chemical Composition of Magnetic Materials. Relative permeabilities μ_r of magnetic materials are very much larger than that of nonmagnetic ones, usually in the order of 10^2 to 10^4. Therefore, the magnetic parameter becomes the major factor in eddy current testing for magnetic materials.

Magnetization (B–H) curves of magnetic materials are chemical composite dependent (15). For example, the curve of carbon steel changes with different carbon content in it, as shown in Fig. 11. Generally, magnetic permeability, residual magnetization, and saturation flux density will all decrease with increasing carbon content. We can use these relationships between magnetic parameters and chemical composites and their contents to evaluate qualities of materials.

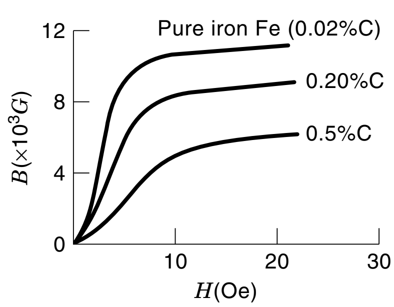

Figure 11. Effect of carbon content in carbon steel on magnetization curves (annealed condition).

Displacement and Vibration Measurement

Displacement Measurement. Generally, the surface-mounted probe, or pancake-type coil, is acceptable for displacement measurement. Parameters of the coil such as diameters, turns, and thickness are required for test range and accuracy. For instance, in order to measure large displacement, a coil with the necessary axial uniform distribution of magnetic field is needed to form a large linear range. If high sensitivity is needed, the variation of eddy current dissipations with the relative movement of coil and testpiece along the coil axis should be large enough, thus a little bit thicker coil is suitable.

Once the conductivity σ, permeability μ, and exciting frequency f have been selected, coil impedance is only the function of distance x between coil and testpiece, as per the lift-off (or "clearance") effect stated earlier. In flaw detecting, however, lift-off effect is an interference factor and needs to be avoided. Curves of lift-off effect are expressed as impedance variation with spacing under conditions of specific materials measured and constant testing frequency, whereas the impedance of a surface-mounted coil is of great significance to lift-off effect. Figure 12 shows an impedance diagram of surface-mounted coils.

Here we should point out that the curves in Fig. 12 were obtained with testing frequency equal to 60 kHz and validated with the test coil only. Coil impedance diagrams will differ when using different coils, different exciting frequencies, and different materials. Thus, these diagrams cannot be for common use but rather for reference. Because the scope of a magnetic field generated by a coil carrying ac current is limited and only its uniform range is usable, linear range of displacement conventionally takes $\frac{1}{3}$ to $\frac{1}{5}$ of the outer diameter of the coil.

Vibration Measurement. Vibration problems are always present in operations of rotational machinery. Serious vibra-

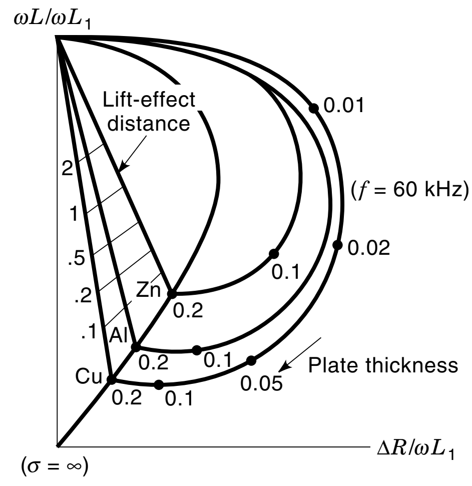

Figure 12. Normalized impedance diagram for surface-mounted coil (or pancake coil).

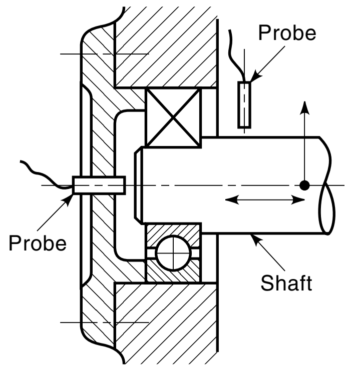

Figure 13. Vibration measurement of rotating shaft.

tions will affect normal operations, so that vibration measurement becomes an important aspect of engineering. The eddy current method serves as a noncontact detecting technique for testing various vibrations.

The testing process is very simple. As long as we place a surface-mounted coil facing the vibrating body within a certain distance from the body, while the vibrating body has reciprocating movements in repeating patterns, the distance between them will be altered periodically, and so will the magnitude of the coil impedance. Testable range of vibration magnitude is generally within several millimeters. The vibration signal can usually be input to an oscilloscop so that its waveshape can be observed directly. Figure 13 shows radial and axial vibration measurements for a turning shaft.

Eddy current methods based on the lift-off effect also have wide use in research activities and industrial processes such as thickness measurement, rotatory angle and rotatory speed measurement, and counting of products.

PROSPECTIVE DEVELOPMENT OF EDDY CURRENT TESTING

In the early 1950s, Förester put forward an "impedance analysis method"—a new way to discriminate various factors that affect eddy current signals. Since then, eddy current testing technology has achieved an essential breakthrough and has come into a new period of practical applications. After the 1970s, the rapid advances in integrating electronics, computer science, and signal processing encouraged the development of eddy current testing and pushed forward theoretical study, practical research, and new equipment production (2). Its application is constantly growing.

Multifrequency Eddy Current Technology

The application of multifrequency eddy current testing is relatively new. After thorough analysis of electric magnetic theory, Libby pointed out that a variety of interference signals can be significantly rejected and valuable signals more easily acquired by means of multifrequency eddy current testing methods. Now, multifrequency technology has been applied to tube flaw detecting, graphic display of tube cross sections, thickness measurement of multilayer metal film, and more (16), even though it isn't widely used yet owing to limitations of component performance, analytical methods for particular problems, complicated circuits, and so on. However, with the development of eddy current theory and computer-based signal processing, the multifrequency method will certainly play an important part in eddy current testing because of its attractive advantages.

Remote Field Eddy Current Testing Technology

The *remote field* method is a low-frequency eddy current technology (17) with which magnetic flux is able to penetrate metallic plates or tubular walls. The eddy current probe for tube flaw detecting works with an exciting coil and a relatively small searching coil that is installed apart about twice that of inner diameter from the exciting coil. The search coil can pick up the magnetic flux that comes from the exciting coil penetrating the tube wall and then returning into the tube. Thus flaws within the inner walls of tubes and decreasing thicknesses of tubular walls can be effectively detected. Because remote field technology has high sensitivity to metal tubes (especially to ferromagnetic tubes), it has become a practical way to inspect various flaws in tubes having long lengths. For that reason, remote field technology has been widely applied to tubes for petroleum, natural gas, and municipal coal gas transporting.

Evaluation of Surface Quality of Metallic Materials

As mentioned before, the eddy current effect is very sensitive to electromagnetic conditions in surface layers of metallic materials. Through the study of relationships between eddy current effects and surface layer performances, the evaluations of surface qualities of metallic materials can be fairly well achieved (9). Therefore we expect that the extensive studies of eddy current testing for residual stress, fatigue cracks, and crack extension and initiation will advance at a great pace.

Computer-Aided Eddy Current Testing

In order to raise reliability and automation of eddy current testing, digital and intelligent instruments have been developed. Numerical calculation for complicated theory problems of eddy current testing will be realized with the most advanced computer technology. Computer technology will be widely used for automatic control and data processing of eddy current testing (18). Microprocessor-based intelligent testing apparatuses that are portable, multifunctional, and easily operated will be emerging.

Signal Image Processing and Discrimination

In eddy current testing, the eddy current information caused by flaws can be extracted by multifrequency technology, after which a variety of images relative to eddy current data can be analyzed by means of computer image processing. Once the images reflecting flaws of tested objects are displayed on screen, the flaws are shown visibly and can be quantitatively analyzed.

Probe Research

The eddy current probe, as pointed out earlier, plays an important role in eddy current testing activities. Its performance mainly comprises linearity, sensitivity, resolution, range, copper resistance, temperature stability, reliability, and probe dimensions. Most of these are connected with probe construction parameters such as coil turns, inner and outer diameters, coil thickness or length, whether air-cored or ferrite-cored, stranded wire-wound coil or metal film-type coil, and the combined use of multiple coils. Consequently, optimum design of probe parameters has become an important project (19). However, there is still a lack of theoretical analysis for probe design. The design is frequently carried out by means of experiment and experience. Optimum design is important, since, for example, a well-built stranded wire-wound coil can reject or reduce temperature drift over a wide temperature range if it is made with the proper diameter of single wire, the correct number of wire strands, and with the proper choice of ac frequency (20).

In short, with the development of science and industrial technology, the theoretical study of eddy current testing and improvement of testing equipment will certainly advance to a new stage. Eddy current testing technology has splendid applications in the fields of aircraft (21), navigation, metallurgy, machinery, electric energy production, chemistry, nuclear power generation, and more.

BIBLIOGRAPHY

1. R. Halmshaw, *Non-destructive Testing,* London: Edward Arnold Publisher, 1987.
2. P. E. Mix, *Introduction to Nondestructive Testing, a Training Guide,* New York: Wiley, 1987.
3. NASA SP-5113, *Nondestructive Testing—A Survey.* Washington, D.C.: National Aeronautics and Space Administration, NASA SP-5113, 1973.
4. H. L. Libby, *Introduction to Electromagnetic Nondestructive Test Methods,* New York: Wiley—Interscience, Wiley, 1971.
5. R. Ji-lin, *Electromagnetic Nondestructive Testing,* Beijing, Aviation Industry Press (China), 1989.
6. B. Hull and V. John, *Non-destructive Testing,* Houndmills, Basingstoke, Hampshire, and London: Macmillan Education Ltd, 1988.
7. R. S. Sharpe, *Research Techniques in Nondestructive Testing,* Volume V, London: Academic Press Inc., 1982.
8. H. Berger, ed., *Nondestructive Testing Standards—A Review,* American Society for Testing and Materials, Philadelphia, 1977.
9. C. O. Roud and R. E. Green, eds., *Nondestructive Methods for Material Property Determination,* New York: Plenum Press, 1984.
10. F. Förester and H. Breitfeld, *Z. Metallkunde,* **45** (4): 1954.
11. C. V. Dodd and W. E. Deeds, *J. Appl. Phys.,* **39** (6): 1968.
12. G. Van Drunen and V. S. Cecco, Recognizing limitations in eddy current testing, *NDT: International,* **17** (1): Feb. 1984.
13. M. D. Halliday and C. J. Beevers, The sizing and location of small cracks in holes using eddy current, *NDT,* **21** (3): June 1988.
14. J. Blitz, D. J. A. Williams, and J. Tilson, Calibration of eddy current test equipment, *NDT International,* **14** (3): June 1981.
15. B. M. Ma and Y. L. Liang, et al., The effect of Fe content on the temperature dependent magnetic properties of Sm (Co, Fe, Cu, Zr) and Sm sintered magnets at 450°C, *IEEE Trans. Magn.* **32** (5): Sept. 1996.
16. J. Blitz and T. S. Peat, The application of multifrequency eddy current testing ferromagnetic metals *NDT International,* **14** (1): Feb. 1981.
17. S. M. Haugland, Fundamental analysis of the remote-field eddy current effect. *IEEE Trans. Magn.* **32** (4): July 1996.
18. T. Stepinski and N. Maszi, Conjugate spectrum filters for eddy current signal processing, *Material Evaluation* (USA) **51** (7): July 1993.
19. A. Powell and T. Meydan, Optimization of magnetic speed sensors, *IEEE Trans. Magn.* **32** (5): Sept. 1996.
20. X. B. Zhuge and B. M. Ling, Analysis of temperature drift rejection of coil impedance, *IEEE Instrumentation and Measurement Technology Conference* **1**: 1996.
21. G. L. Fitzpatrick et al., Magneto-optic/eddy current imaging of aging aircraft: A New NDI Technique, *Material Evaluation* (USA) **5** (12): Dec. 1993.

XIANGBIN ZHUGE
Zhejiang University
BAOMING LING
Zhejiang University

EDUCATION. See COMPUTER ENGINEERING EDUCATION; EDUCATIONAL TRENDS; ELECTRICAL ENGINEERING EDUCATION; MANAGEMENT EDUCATION; PROFESSIONAL PREPARATION.